HEFAT2014
10th International Conference on Heat Transfer, Fluid Mechanics and Thermodynamics
14 – 16 July 2014
Orlando, Florida

EXPERIMENTAL ANALYSIS OF GAS TO WATER TWO PHASE CLOSED THERMOSYPHON BASED HEAT EXCHANGER

Ramos, J.B.[1], Chong, A.[1], Tan, C.[1], Matthews, J.[1], Boocock, M.A.[2], Jouhara, H.[2]
[1]University of South Wales, Faculty of Advanced Technology,
Trefforest, CF37 1DL, UK, E-mail: joao.ramos@southwales.ac.uk
[2]Econotherm (UK) Ltd, an associate company of Spirax-Sarco Engineering plc,
Waterton Rd, Bridgend, CF31 3YY, UK, E-mail: hussam.jouhara@econotherm.eu

ABSTRACT

Wickless heat pipes have been attracting increased attention in the last two decades due to their reliability and high heat transfer potential per unit area. Their most common application is in the process industry, when coupled to waste heat recovery devices. Heat pipe based heat exchangers offer many advantages when compared with conventional waste heat recovery systems; advantages that are detailed in the current work. The design of such devices, however, is not a straightforward process due to the complex modes of heat transfer mechanisms involved. In this paper, the characterisation of a cross-flow heat pipe based heat exchanger is studied experimentally, using correlations currently available in literature. A design tool with the purpose of predicting the performance of the test unit was also developed and validated through comparison with the experimental results. The design tool was validated with the use of a purpose-built experimental facility.

Keywords: *heat recovery, heat exchangers, heat pipes, thermosyphons, effectiveness*

INTRODUCTION

Waste heat recovery is a growing area in industry. This recent growth is a direct result of tighter environmental policies instigated by the Kyoto Protocol [1,2]. Present heat recovery systems have to be safe, efficient and economical in order to be justifiable in today's competitive market. Of all the ideas and designs available, heat pipe based systems are desirable due to their increased reliability, ease of operation, system efficiency and reduced manufacturing cost. The reliability is provided by their passive operation and flow separation, and the reduction in cost is a result of recent advances in manufacturing methods. Due to their mode of operation through evaporation and condensation of an internal fluid, heat pipes have been described as super thermal conductors [3,4], as the phase change process is able to transport heat energy at a much higher rate than pure conduction through a solid.

Heat pipes are known for their adaptability, having a proven track record in a wide range of different areas, namely space applications [5], computer and electronics [6], ventilation and air conditioning [7-9], heating systems [10,11], solar energy systems [12], water desalination [13] and nuclear energy [14]; but perhaps the most promising incorporation of heat pipe technology is in waste heat recovery for industrial applications.

An extensive amount of literature is available on heat pipes being used in air handling units at low temperatures (<100 ^{o}C), but it is quite scarce for higher temperatures, (100 ^{o}C < T < 300 ^{o}C). Waste heat recovery units can have multiple uses: pre-heating incoming air, maintaining a fluid at a high temperature, generating steam, or space heating.

NOMENCLATURE

A	[m^2]	Heat Transfer Area
c_p	[J/(kg.K)]	Specific heat capacity
C	[W/K]	Heat Capacity Rate
C_r	[-]	Heat Capacity Ratio
FR	[m^3/s]	Flow Rate
h	[W/m^2.K]	Heat Transfer Coefficient
$\dot{m}$	[kg/s]	Mass Flow Rate
$\dot{Q}$	[W]	Heat Transfer Rate
R	[K/W]	Thermal Resistance
T	[^{o}C]	Temperature
ΔT	[^{o}C]	Difference in Temperature
U	[W/m^2.K]	Overall Heat Transfer Coefficient
ε	[-]	Effectiveness

Subscripts

a	Air
av	Average
c	Condenser side / Cold side
e / h	Evaporator side / Hot side
hp	Heat pipe / Thermosyphon
i	Inlet
n	Number of pipes
o	Outlet
w	Water

Abbreviations

NTU	Number of Transfer Units
HPHE	Heat pipe Heat Exchanger

A heat pipe heat exchanger can be described as an indirect-transfer heat exchanger relying solely on the evaporation and condensation of the working fluid to transfer heat [4]. It usually consists of an array of straight heat pipes arranged vertically; the pipes are swept by a hot flow in their lower section and a cold flow in the upper section. They will passively absorb heat from the hotter medium and release it in the colder stream through the constant evaporation and condensation of the

working fluid inside the pipe. One of the requirements of a working heat pipe is a temperature difference between the streams that the heat pipe is exposed to at each of its ends [15].

The heat extraction behaviour of a heat pipe based heat exchanger is highly dependent on the flow configuration and conditions. Therefore, a detailed experimental study is required in order to characterise the performance of the system [16].

Due to the complex nature of the heat transfer mechanisms in the pipes and their interaction with their fluid environments, an experimental investigation is proposed for a specific heat exchanger configuration.

The thermal resistance analogy is a well-known method for characterisation of a heat exchanger using experimental data. It consists of comparing the heat exchanger to an electrical circuit and turning all modes of heat transfer into resistances. This method is further complemented by the use of the Effectiveness [17,18], a variable often used in the characterisation of heat exchangers and a great tool when generating numerical prediction models.

This paper describes the characterisation of an air-to-water heat pipe-equipped heat exchanger. The evaporator inlet conditions, such as temperature and mass flow rate, are manipulated, and the heat extraction profile is investigated, assuming the heat pipes have a constant thermal resistance. The resistance to heat transfer offered by the heat pipes is then related to the Effectiveness of the heat exchanger.

TEST FACILITY DESIGN

The experimental rig consisted of a heat exchanger equipped with six heat pipes in a cross-flow arrangement. The design of the rig was based on a real working example of a larger heat exchanger. The test facility was composed of two parts: a hot air circuit and a cold water circuit. The hot air circuit was a closed loop propelled by a fan. The cold water circuit was controlled by a simple ball valve, as can be seen in Figure 1.

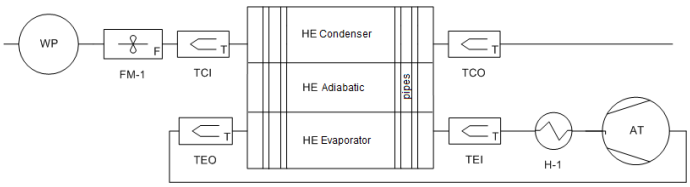

Figure 1 Schematic of the test setup. Description: WP – Water pump; FM-1 – Turbine Flow Meter; TCI/TCO – Thermocouple at inlet/outlet of condenser; HE-C/E – Heat pipe heat exchanger Condenser/Evaporator; TEI/TEO – Thermocouple at inlet/outlet of evaporator; H-1 – Air Heater; AT – Air Turbine

The hot air flow consisted of a single pass sweeping all 6 pipes at a time. The mass flow rate was controlled by a fan. The temperature was measured by a K-type thermocouple located at the inlet of the evaporator section which also controlled the power of the air heater. The data was gathered using a 32-channel data logging device connected to an array of K-type thermocouples. These thermocouples were placed in specific locations within the heat exchanger in order to provide information on the flow, and the heat pipe's surface and interior temperature.

TEST PIECE DESIGN

In order to have a better working understanding of the heat pipe heat exchanger, it is customary to divide it in three sections. The bottom section is in contact with the hot air stream and is named Evaporator; here the heat energy supplied to the heat pipes causes the internal working fluid to evaporate. The top section where the cold water stream flows is termed Condenser; here the heat is removed from the heat pipes, causing the working fluid within the pipes to condense and flow back to the bottom, aided by the force of gravity. The middle section is termed Adiabatic since there is no heat transfer taking place.

The condenser section occupied the top 0.2 m of the pipes, and the evaporator section covered the lower 0.6 m. Both sections were separated from the adiabatic section by a 10 mm-thick division plate in order to prevent leaks. The flow inside the condenser consisted of a u-shaped path (please see Figure 2) and a bleeding valve was installed on the top of the condenser to remove all the air from the section when initiating operation.

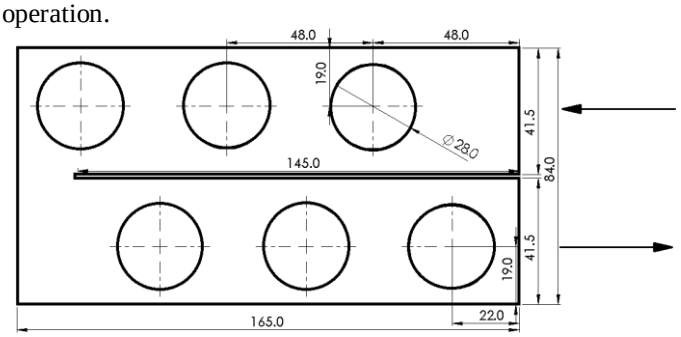

Figure 2 Cross-section of the Condenser part of the Heat Exchanger (all dimensions in mm)

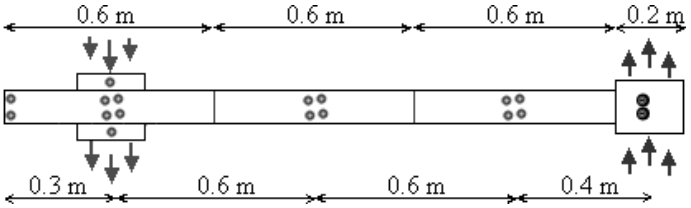

Figure 3 Representative schematic of the heat pipe heat exchanger and thermocouple placements (represented by the circles)

The thermocouples were placed in key sections; namely at each inlet and outlet of both the hot flow and the cold flow, on the surface of each pipe, in the adiabatic section, and within the heat pipes. The thermocouple placements can be seen in Figure 3, represented by the circles. The thermocouples in the pipes were located in the base of the heat pipes.

The six heat pipes were all made of carbon steel, measured 2 meters in length and had a diameter of 28 mm. The surrounding wall of the heat pipes had an average thickness of 2.5 mm. The working fluid was distilled water, filled to a third of the total volume. All the pipes were chemically treated before insertion of water in order to avoid corrosion.

HEAT EXCHANGER EFFECTIVENESS MODEL

Through the data gathered, a numerical effectiveness model can be developed in order to predict the effectiveness of the heat exchanger. In order to develop the model, the entire system is divided into two separate heat exchangers with the working fluid as the division between them. The effectiveness is the ratio of the actual heat transfer rate to the maximum theoretical heat transfer rate and if the results are available, it is determined from the following expression:

$$\varepsilon = \frac{\dot{Q}_{actual}}{\dot{Q}_{max}} = \frac{C_w(T_{c,o}-T_{c,i})}{C_{min}(T_{max}-T_{min})} = \frac{C_w(T_{c,o}-T_{c,i})}{C_{min}(T_{h,i}-T_{c,i})} \quad (1)$$

Where $\dot{Q}$ represents the heat transfer rate, C_w refers to the heat capacity rate for water (w) and C_{min} represents the minimum heat capacity rate between the water side and the air side. T_c refers to the cold side and T_h to the hot side. The heat transfer rate is usually determined through the equation:

$$\dot{Q} = \dot{m} c_p \Delta T \quad (2)$$

In this equation $\dot{m}$ represents the mass flow rate (kg/s), c_p the specific heat capacity (J/(Kg.K)) for the fluid in question and ΔT (^{o}C or K) the difference in temperature between the inlet and the outlet of a given section.

However, the effectiveness can also be related to the Number of Transfer Units. The general formula for the effectiveness in each side of the heat exchanger is the following [18]:

$$\varepsilon = \frac{1-e^{[-\mathrm{NTU}(1-C_r)]}}{1-C_r \cdot e^{[-\mathrm{NTU}(1-C_r)]}} \quad (3)$$

The expression above refers to either the heat being transferred from the hot flow to the working fluid inside the heat pipe or to the heat transfer from the working fluid to the cold flow. C_r is the ratio between the heat capacity rates of the shell-side fluid and the working fluid inside the pipe (C_{min}/C_{max}). The working fluid inside the pipe, however, is in a constant state of evaporation on the hot side and of condensation on the cold side, which results in an incredibly high value of the heat capacity rate (C). Since the heat capacity rate for the fluid in phase change is far superior to the fluid on the shell side, the ratio of heat capacity rates (C_r) is assumed to be zero. Assuming $C_{min}/C_{max} \approx 0$ we are left with an expression of effectiveness for each side of the heat exchanger:

$$\varepsilon_h = 1 - e^{(-\mathrm{NTU}_h)} \quad (4)$$

$$\varepsilon_c = 1 - e^{(-\mathrm{NTU}_c)} \quad (5)$$

The Number of Transfer Units (NTU) is a method of presenting mean temperature differences, and it is the relation between the overall heat transfer coefficient (U), the total heat transfer area (A) and the minimum Heat Capacity Rate (C_{min}) like so:

$$\mathrm{NTU}_h = \frac{U_h A_h}{C_h} \quad (6)$$

$$\mathrm{NTU}_c = \frac{U_c A_c}{C_c} \quad (7)$$

The heat transfer coefficient is then related to the local heat transfer coefficients (h_x), the Area of exposure to the flow and the heat pipe's inner resistance to temperature change.

$$\frac{1}{U_h A_h} = \frac{1}{h_h A_{hp}} + R_{hp,h} \quad (8)$$

$$\frac{1}{U_c A_c} = \frac{1}{h_c A_{hp,c}} + R_{hp,c} \quad (9)$$

The method to determine the internal resistances of the thermosyphon is made available by the Engineering Sciences Data Unit (ESDU) [19].

Additionally, the effectiveness of a single heat pipe can be found from the following equation by Faghri [20]:

$$\varepsilon_p = \left(\frac{1}{\varepsilon_{min}} + \frac{C_r}{\varepsilon_{max}}\right) \quad (10)$$

C_r is the ratio of Heat Capacity rates (C_{min}/C_{max}) within the heat pipe and ε_x are the maximum and minimum values of effectiveness for each of the sides (evaporator and condenser). The expression below is required in order to determine the effectiveness of the entire heat exchanger [18]:

$$\varepsilon = \frac{\left(\frac{1-\varepsilon_p C_r}{1-\varepsilon_p}\right)^n - 1}{\left(\frac{1-\varepsilon_p C_r}{1-\varepsilon_p}\right)^n - C_r} \quad (11)$$

This is, coincidentally, the equation used on a shell and tube heat exchanger with n passes. In the original equation, ε_p represents the effectiveness for a single pass; it is only logical that in order to incorporate heat pipes the effectiveness of a single pipe is used. In this case, however, the superscript n represents the number of rows of heat pipes in the direction of air flow. The ratio of heat capacity rates (C_r) in the equation above refers to the different heat capacity rates in the shell side fluid of the evaporator and the condenser [21]. The effectiveness determined through equation (11) can then be used to determine the heat transfer rate through the following expression:

$$\dot{Q} = \varepsilon \cdot \dot{Q}_{max} \quad (12)$$

Going back to equation (1), the maximum heat extraction rate can be found by multiplying the minimum heat capacity rate by the maximum difference in temperature, which in this case is the difference between the inlet temperatures:

$$\dot{Q}_{max} = C_{min}(t_{h,i} - t_{c,i}) \quad (13)$$

Through manipulation of the equation above, the outlet temperatures can be predicted through equations (14) and (15) below:

$$T_{h,o} = T_{h,i} - \frac{\dot{Q}}{C_h} \quad (14)$$

$$T_{c,o} = T_{c,i} + \frac{\dot{Q}}{C_c} \quad (15)$$

The iterative thermal balancing technique used in the empirical model makes use of the known parameters of inlet temperatures and air flow rates. The main assumption is that all the thermosyphons have the same value of overall thermal resistance: an average value derived from the experimental data. This iteration is based on the law of conservation of energy, and only possible if it is assumed that there are no losses in the adiabatic section. Therefore the thermal resistance offered by a single heat pipe is the inverse of the heat transfer rate:

$$R_{hp} = \frac{T_{e,av} - T_{c,av}}{Q_{hp}} \quad (16)$$

OPERATIONAL PROCEDURE

In order to investigate the thermal performance of the heat exchanger, a number of tests were performed. The temperature in the hot air stream ranged from 50 °C to 300 °C at 50 °C increments, and the mass flow rate varied between 0.05 kg/s and 0.2 kg/s at approximately 0.035 m^3/s increments, a result of the fan setting from 10 Hz to 50 Hz. In the cold section, the mass flow rate was a constant 7.16×10^{-2} m^3/s at an average temperature of 10 °C. All the tests were run for a minimum of 9 minutes at steady state, as can be seen in Table 1.

Table 1 Testing time for each variable (at s.s., in minutes)

Hz\°C	50 °C	100 °C	150 °C	200 °C	250 °C	300 °C
10 Hz	09:05	08:45	08:35	10:40	08:41	09:18
20 Hz	09:01	08:37	08:31	08:57	09:02	08:21
30 Hz	10:00	08:15	08:21	09:02	08:28	10:30
40 Hz	09:21	10:56	10:53	11:13	14:40	08:13
50 Hz	10:23	16:11	11:23	10:05	09:40	07:11

The cold flow was kept at essentially constant temperature and its variation is presented in Table 2. The mass flow rate was also kept at a constant rate of 7.16×10^{-2} m^3/s throughout all the experiments.

Table 2 Comparison between inlet temperatures

Average inlet temperature of Evaporator (air)	Average inlet temperature of Condenser (water)
300 °C	10.3 °C
250 °C	9.8 °C
200 °C	10.2 °C
150 °C	10.0 °C
100 °C	9.7 °C
50 °C	9.7 °C

RESULTS AND DISCUSSION

The total heat extraction duty of the system was determined with the equation $\dot{Q} = \dot{m} c_p \Delta T$. To determine the heat transfer rate, the characteristics of the water side were used in the calculation.

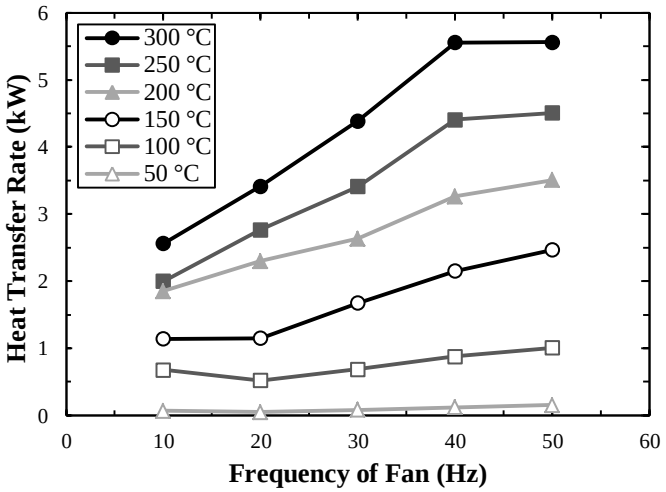

Figure 4 Power output according to Inlet temperature and mass flow rate

The value of the heat transfer rate (Q) was found for every temperature and frequency of fan combination, as can be seen in Figure 4. A pattern occurs for all inlet temperatures: the heat transfer rate increases steadily with an increasing flow rate, and then a "plateau" is reached from 40 Hz to 50 Hz. The "plateau" is a result of the constant mass flow rate on the cold side having reached its saturation point and not being able to absorb any more heat energy. At higher temperatures (200 – 300 °C), the power output seems to be quite similar, following a steady trend.

The temperature distribution profiles can be seen in Figure 5. Here, higher mass flow rates on the hot air side seem to result in smaller temperature differences between the inlet and the outlet of the evaporator, and also higher temperature differences between the inlet and the outlet of the condenser, which is to be expected. According to the charts, the temperature of the adiabatic section suffers a slight fluctuation. This fluctuation is explained by the thermocouples' placements; the adiabatic section is a hollow box and the thermocouples are in contact with the air contained inside this box. Due to the insulation covering the adiabatic section, whenever the temperature or the mass flow rates of the shell-side fluids are changed, the heat energy is kept within, delaying the response of the thermocouples.

The resistance to heat transfer offered by the heat pipe bundle has also been plotted for each different set of data and is presented in Figure 6. A pattern seems to emerge in which higher inlet temperatures have a comparatively lower value of resistance. The resistance is very high at inlet temperatures of 50 °C, (0.3 – 0.8) and that is due to reduced performance of the heat pipe at lower temperature differences between the two streams.

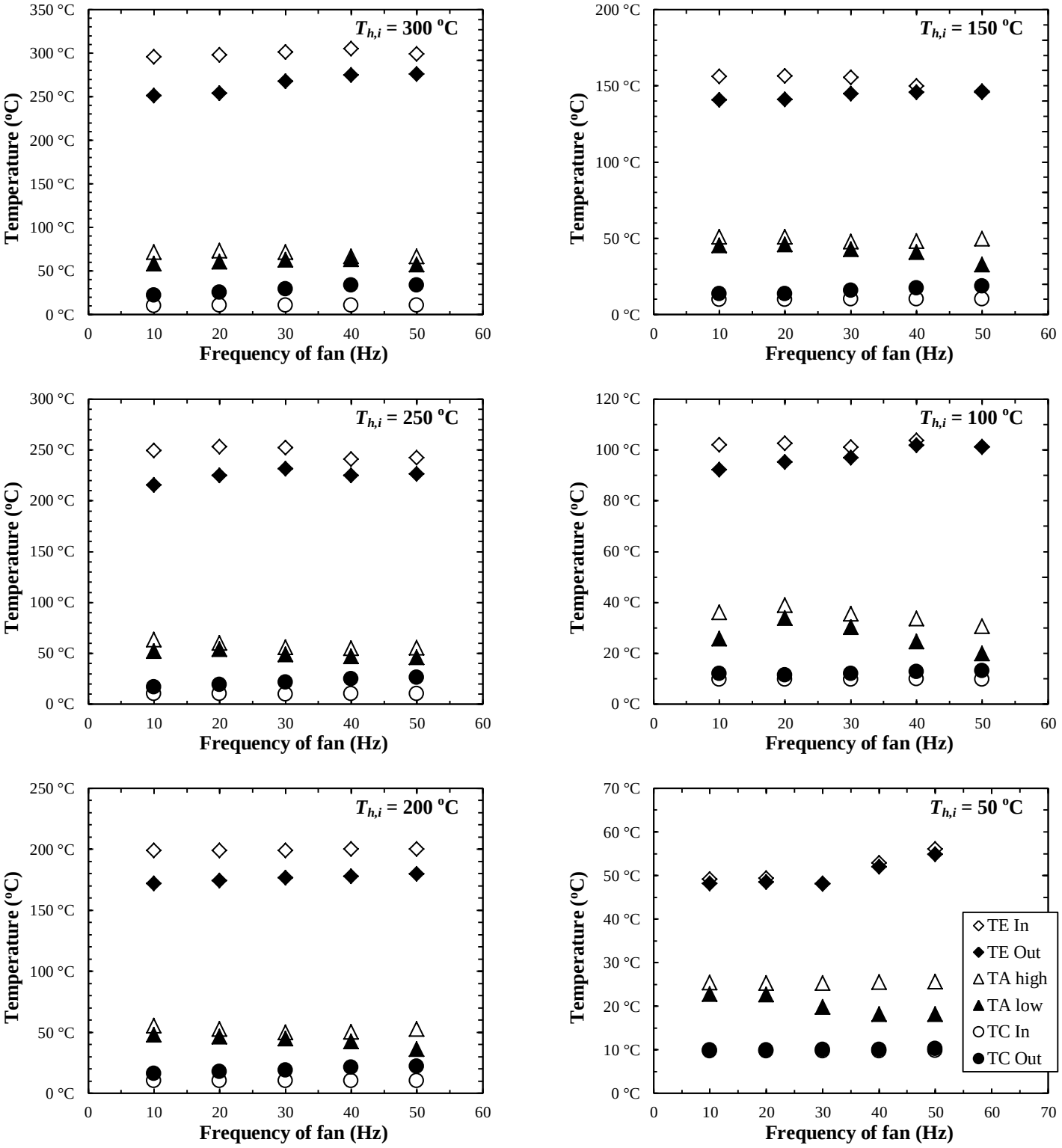

Figure 5 Temperature distribution profiles through the HPHE at various power throughputs. TE – Temperature in the Evaporator Section; TA – Temperature in the Adiabatic Section; TC – Temperature in the Condenser Section

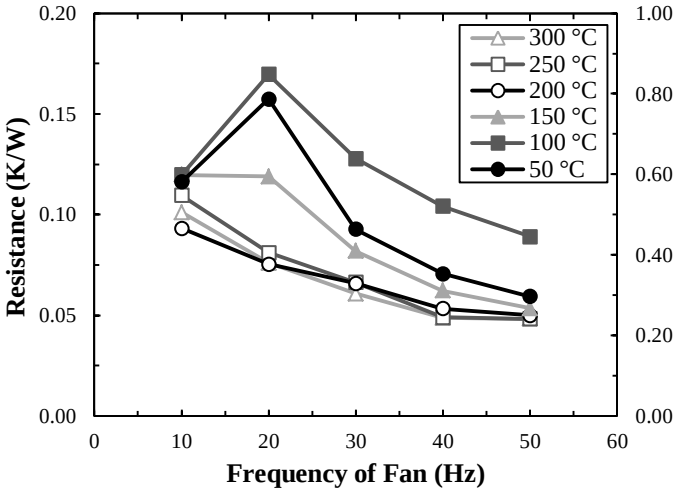

Figure 6 Thermal Resistance of the heat exchanger in relation to the flow conditions at the inlet of the hot air flow (The results for 50 °C are represented in a different scale)

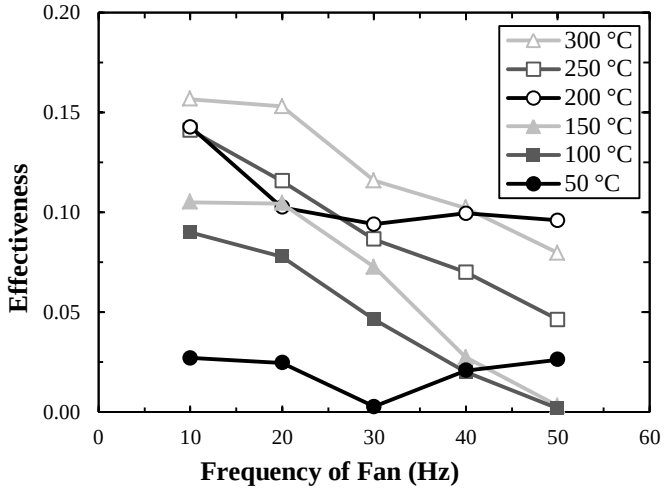

Figure 7 Effectiveness of Heat Exchanger according to different fan frequencies and temperatures

The effectiveness of the heat exchanger exhibits a constant downward trend as the mass flow rate of the hot air increases. This is a direct result of the reduction in the time spent by the hot air within the proximity of the heat pipes.

A constant downward slope can be seen for the effectiveness of all the temperature profiles, which is the result of having a constant mass flow rate in the cold side, limiting the heat absorption potential of the condenser. The tests done at 50 °C and 200 °C do not follow the normal downward trend. The irregularity in 50 °C tests does not come as a surprise as the uncertainty values are relatively high for this test (please refer to Table 3) and the Thermal Resistance (Figure 6) is the highest among all the tested mass flow rates. As for the experiments made at 200 °C a possible explanation could be that a sudden increase in the mass flow rate of the cold side was not reflected in the experimental data.

ERROR ANALYSIS

The main source of uncertainty for the calculated effectiveness values in Equation (12) came from the temperature measurements of $T_{c,i}$ and $T_{c,o}$, obtained using K-type thermocouples (NiCr/NiAl) and a data logger (DataScan). The uncertainties for K-type thermocouples are estimated to be ±0.05% rdg + 0.3 °C.

The propagation of uncertainties associated with the calculated effectiveness values can be calculated from:

$$S_\varepsilon = \varepsilon \cdot \sqrt{\left(\frac{S_{Q_c}}{Q_c}\right)^2 + \left(\frac{S_{C_a}}{C_a}\right)^2 + \left(\frac{S_{\Delta T_{max}}}{\Delta T_{max}}\right)^2} \qquad (17)$$

Where,

$$S_{Q_c} = Q_c \cdot \sqrt{\left(\frac{S_{FR_w}}{FR_w}\right)^2 + \left(\frac{S_{\Delta T_c}}{\Delta T_c}\right)^2} \qquad (18)$$

$$S_{\Delta T_{max}} = \sqrt{\left(S_{T_{h,i}}\right)^2 + \left(S_{T_{c,i}}\right)^2} \qquad (19)$$

$$S_{\Delta T_c} = \sqrt{\left(S_{T_{c,o}}\right)^2 + \left(S_{T_{c,i}}\right)^2} \qquad (20)$$

Table 3 presents the maximum experimental uncertainty which was more prominent at lower temperatures and mass flow rates.

Frequency	300 °C	250 °C	200 °C	150 °C	100 °C	50 °C
10 Hz	8.11%	9.98%	10.74%	16.83%	*3832.96%*	*277.74%*
20 Hz	6.57%	7.80%	8.21%	16.69%	*36.05%*	*371.65%*
30 Hz	5.77%	7.03%	7.11%	12.56%	*29.22%*	*496.06%*
40 Hz	5.25%	6.56%	6.88%	16.65%	*33.95%*	*160.39%*
50 Hz	5.54%	6.27%	5.99%	*125.52%*	*317.47%*	*125.64%*

Table 3 Maximum Uncertainty for Effectiveness (%)

In engineering applications, 10% is usually considered an acceptable value of uncertainty [22]. As can be seen in Table 3, there is a high degree of uncertainty related to the experiments carried out at lower temperatures (represented in Italics); however this is to be expected, as the heat capacity rate of the air side was deduced from the data gathered in the cold side. Furthermore, heat pipes with water as a working fluid are known to perform less efficiently at lower temperatures.

CONCLUSION

An air-to-water heat exchanger equipped with heat pipes was investigated experimentally for a range of inlet flow conditions in the evaporator side. The effectiveness and its relation to the heat transfer rate and the temperature profile have also been determined within the constraints imposed by the experimental rig. The heat transfer rate for the heat exchanger exhibits a constant upward trend as the mass flow rate of the hot air increases. It is only limited at its maximum value by a combination of the inability of the cold water to absorb more heat and the hot air not being allowed enough time in the vicinity of the pipes to transfer the heat conserved within. Although the heat transfer rate increases with increasing mass flow rates, the effectiveness of the heat exchanger exhibits a constant downward trend, as explained before, a result of the

hot air not being having enough time to transfer its heat to the pipes. There is lower uncertainty at higher temperatures, which also reveal a higher overall effectiveness and heat transfer rate as well as lower resistance to heat transfer. The experimental results were in accordance with the numerical approach for shell-and-tube heat exchangers based on current literature, demonstrating that heat pipe equipped heat exchangers may be characterised through the same methods as shell-and-tube heat exchangers by considering the heat pipes as solid objects of constant thermal resistance. It is advised that the tests should be repeated in a more controlled environment in order to reduce the level of uncertainty. Additionally, the effect of the manipulation of the flow characteristics on the water side could be further explored as it was not on the scope of the experiment.

ACKNOWLEDGEMENTS

Special thanks are due to Mr Stefan Munteanu and Mr Peter Blackwell for the fast and flawless way they got the rig ready for experimentation. Thanks are also due to Mr Michael Jones for having helped with the maintenance and technical support.

REFERENCES

[1] United Nations. Kyoto Protocol. 11-12-1997.
[2] Hansen J., Sato M., Ruedy R., Lo K., Lea D.W., and Medina-Elizade M., Global temperature change, *Proceedings of the National Academy of Sciences*, 103 (2006) 14288-14293.
[3] Yang X., Yan Y.Y., and Mullen D., Recent developments of lightweight, high performance heat pipes, *Applied Thermal Engineering*, 33-34 (2012) 1-14.
[4] Jouhara H., and Ezzuddin H., Thermal performance characteristics of a wraparound loop heat pipe (WLHP) charged with R134A, *Energy*, 61 (2013) 128-138.
[5] Dong S.J., Li Y.Z., and J. Wang, Fuzzy incremental control algorithm of loop heat pipe cooling system for spacecraft applications, *Computers & Mathematics with Applications*, 64 (2012) 877-886.
[6] Wang J.C., 3-D numerical and experimental models for flat and embedded heat pipes applied in high-end VGA card cooling system, *International Communications in Heat and Mass Transfer*, 39 (2012) 1360-1366.
[7] Jouhara H., and Robinson A.J., An experimental study of small-diameter wickless heat pipes operating in the temperature range 200C to 450C., *Applied Thermal Engineering*, 30 (2011) 1041-1048.
[8] Chaudhry H.N., Hughes B.R., and Ghani S.A., A review of heat pipe systems for heat recovery and renewable energy applications, *Renewable and Sustainable Energy Reviews*, 16 (2012) 2249-2259.
[9] Akbarzadeh A., Johnson P., Nguyen T., Mochizuki M., Mashiko M., Sauciuc I., Kusaba S., and Suzuki H., Formulation and analysis of the heat pipe turbine for production of power from renewable sources, *Applied Thermal Engineering*, 21 (2001) 1551-1563.
[10] Wang Z., Duan Z., Zhao X., and Chen M., Dynamic performance of a façade-based solar loop heat pipe water heating system, *Solar Energy*, 86 (2012) 1632-1647.
[11] Zhang X., Zhao X., Xu J., and Yu X., Characterization of a solar photovoltaic/loop-heat-pipe heat pump water heating system, *Applied Energy*, 102 (2013) 1229-1245.
[12] Nithyanandam K., and Pitchumani R., Computational studies on a latent thermal energy storage system with integral heat pipes for concentrating solar power, *Applied Energy*, 103 (2013) 400-415.
[13] Jouhara H., Anastasov V., and Khamis I., Potential of heat pipe technology in nuclear seawater desalination, *Desalination*, 249 (2009) 1055-1061.
[14] Laubscher R., and Dobson R.T., Theoretical and experimental modelling of a heat pipe heat exchanger for high temperature nuclear reactor technology, *Applied Thermal Engineering*, 61 (2013) 259-267.
[15] Wadowski T., Akbarzadeh A., and Johnson P., Characteristics of a gravity-assisted heat pipe-based heat exchanger, *Heat Recovery Systems and CHP*, 11 (1991) 69-77.
[16] Hagens H., Ganzevles F.L.A., van der Geld C.W.M., and Grooten M.H.M., Air heat exchangers with long heat pipes: Experiments and predictions, *Applied Thermal Engineering*, 27 (2007) 2426-2434.
[17] Noie, S.H. Investigation of thermal performance of an air-to-air thermosyphon heat exchanger using e-NTU method, *Applied Thermal Engineering*, 26 (2006) 559-567.
[18] Incropera F., and Dewitt D., Fundamentals Of Heat And Mass Transfer, 4th Ed, John Wiley & Sons, 1996.
[19] ESDU 81038. Heat pipes - performance of two-phase closed thermosyphon, *Engineering Sciences Data Unit*, 1983.
[20] Faghri A. Heat pipe science and technology, Taylor & Francis, 1995.
[21] Jouhara H., and Merchant H., Experimental investigation of a thermosyphon based heat exchanger used in energy efficient air handling units, *Energy*, 39 (2012) 82-89.
[22] Taylor, JR. An introduction to error analysis: the study of uncertainties in physical measurements, University Science Books, 1997.